

Self-calibrating shift-and-add technique for speckle imaging

Julian C. Christou,* E. Keith Hege,† Jonathan D. Freeman, and Erez Ribak

Steward Observatory, University of Arizona, Tucson, Arizona 85721

Received June 3, 1985; accepted September 24, 1985

An image-reconstruction technique for astronomical speckle interferometric data is described. This variant of the shift-and-add algorithm originally developed by Lynds *et al.* [Astrophys. J. 207, 174 (1976)] utilizes a weighted impulse distribution of speckle positions to extract an average speckle for a data set. This is done by means of a weighted deconvolution procedure, similar in form to a Weiner filter, which deconvolves the specklegram by the impulse distribution. Results show that this method appears to be self-calibrating for seeing effects. It yields point-spread functions, for observations of an unresolved star, that compare quantitatively with computed Airy patterns for both simple apertures and the fully phased multiple mirror telescope array. Images of the resolved object Alpha Orionis show evidence of an extended stellar envelope.

INTRODUCTION

Since its introduction by Labeyrie,¹ speckle interferometry has been used to obtain diffraction-limited information about astronomical objects. In its original form the technique yielded the object distribution power spectrum estimate of a series of short-exposure (~60-msec) images (specklegrams). This power spectrum estimate only contains information about the modulus of the Fourier transform of the object distribution and, without the phases of the Fourier transform, cannot be used to reconstruct the object. A number of techniques have been developed to reconstruct these phases and therefore the object by invoking the fact that for measured data sets a unique phase solution exists.²⁻⁴ These techniques, however, rely on no input phase information. Furthermore, the effects of measured noise on the numerical efficiency of the phase-retrieval algorithms, on which these techniques are based, are not as yet fully understood. A number of other imaging techniques exist that recover the phases from the original specklegrams. Among those are the shift-and-add algorithms^{5,6} and the Knox-Thompson⁷ approach. Comprehensive reviews of speckle imaging techniques can be found in work by Bates⁸ and Dainty.⁹

The preferred imaging techniques are those that use the phase information available in the specklegrams. One such set of methods make use of the intuitive interpretation of a speckle as being a highly distorted version of the diffraction-limited image. Variations of this form of analysis were proposed by Lynds *et al.*⁵ and Bates and Cady,⁶ and a theoretical study by Hunt *et al.*¹⁰ has shown that diffraction-limited information is preserved. The latter method, known as shift-and-add (SAA) has been further developed by Bagnuolo.^{11,12} SAA is accomplished by first locating the brightest pixel in each specklegram and then shifting the specklegram to place this pixel at the center of image space. The final image is obtained by averaging over a set of shifted specklegrams. The result is a diffraction-limited image sitting on top of a seeing-produced background, which is produced by averaging over the remaining speckles of the speck-

legram. Thus the SAA image is dependent on the seeing conditions and contains a seeing-dependent bias (background). The Lynds, Worden, and Harvey (LWH) technique utilizes those speckles whose intensities lie above some threshold (typically the brightest 10%) and uses them to generate an impulse distribution of delta functions having unit amplitude at the speckle positions. The LWH image is built up by cross correlating the specklegram with the impulse distribution to shift these brightest speckles to the center of image space. The final result is obtained by averaging over the whole data set. Like the SAA image, the LWH image also comprises two components, the diffraction-limited image on top of a broader seeing background. For both methods the extraction of the diffraction-limited image is dependent on the seeing conditions, and this is made more difficult when the size of the object approaches that of the seeing disk.

METHOD

The technique that we have used is derived from that of LWH but utilizes *all* speckles in the specklegram above a background noise level. The specklegram $i(\mathbf{r})$ is assumed to be approximated by a convolution of the object $o(\mathbf{r})$ with the telescope point-spread function $a(\mathbf{r})$ all convolved with a set of weighted delta functions (impulse distribution), $\text{Imp}(\mathbf{r})$, corresponding to the amplitudes and positions of the speckles, i.e.,

$$i(\mathbf{r}) = [o(\mathbf{r}) * a(\mathbf{r})] * \text{Imp}(\mathbf{r}), \quad (1)$$

where $*$ denotes convolution and \mathbf{r} represents the image domain. This simple model takes into account that the specklegram is formed by random phase shifts in the complex wave front due to refractive-index variations in the atmosphere. Thus a specklegram can be considered to be a set of highly distorted diffraction-limited images within a region defined by the seeing disk. Therefore, if this assumption is true, the diffraction-limited image can be obtained by deconvolving the specklegram by the impulse distribution.

The impulse distribution can be obtained by locating all the speckle maxima and setting the amplitudes of the delta functions equal to that of the corresponding speckle amplitudes. Thus, when the specklegram Eq. (1) is deconvolved by the impulse distribution, the result is, to a first approximation, the diffraction-limited image of the object. In this analysis we used the local maxima in the specklegrams to define the amplitude and position of the impulses.

To avoid the problems inherent in regular deconvolution techniques, i.e., division by zero or small numbers in the complex quotient, we have implemented a weighted deconvolution procedure similar in form to a Wiener filter. Denoting the Fourier transform by uppercase letters, then the complex quotient can be written as

$$FT\{o(\mathbf{r}) \star a(\mathbf{r})\} = \frac{\sum_n [I_n(\mathbf{f})/\text{Imp}_n(\mathbf{f})] W_n(\mathbf{f})}{\sum_n W_n(\mathbf{f})}, \quad (2)$$

where \mathbf{f} is the spatial frequency domain corresponding to \mathbf{r} , n identifies the n th specklegram, and $W_n(\mathbf{f})$ its weighting.

In order to minimize the number of complex divisions and to obtain a function that is always nonzero we chose the weighting function to be the power spectrum of the impulse distribution, i.e., $W_n(\mathbf{f}) = |\text{Imp}_n(\mathbf{f})|^2$. The numerator in Eq. (2) then becomes the cross spectrum between the specklegram and the impulse distribution, thus reducing the number of complex quotients to one, that of the ensemble average (sum) of the cross spectra and the impulse power spectra, so that Eq. (2) can be rewritten as

$$FT\{o(\mathbf{r}) \star a(\mathbf{r})\} = \frac{\sum_n I_n(\mathbf{f}) \text{Imp}_n^*(\mathbf{f})}{\sum_n |\text{Imp}_n(\mathbf{f})|^2}. \quad (3)$$

The averaged impulse-distribution power spectrum contains a bias term due to Poisson statistics and is therefore nonzero at all frequencies. Because we use a weighted impulse distribution and a weighted deconvolution technique we call this analysis weighted shift-and-add/weighted deconvolution (WSA/WD).

It is interesting to note that the numerator of Eq. (3) is the Fourier transform of the cross correlation of the specklegram with the weighted impulse distribution and therefore is a minor modification to the LWH technique, which we denote by WSA/XC.

RESULTS

The WSA images, as well as the images from other SAA techniques, contain a photon spike at the center owing to the photon noise in the specklegrams. This can be removed by a correction applied in the Fourier plane. At the same time, the effects of the detector transfer function can also be removed. Hege *et al.*¹³ have reported that the detector response is a sharp Gaussian. In the spatial frequency domain this becomes a broad Gaussian, which is a multiplicative term because of the convolution of the detector response with the signal. A Gaussian is fitted to frequencies beyond the telescope cutoff $f = D/\lambda$, where D is the diameter of the

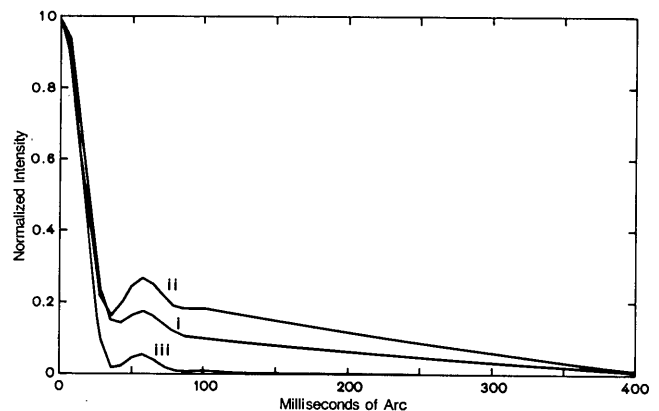


Fig. 1. Radial average profiles for Gamma Orionis: (i) SAA, (ii) WSA/XC, and (iii) WSA/WD at $\lambda = 650.0/0.2$ nm using the KPNO 4-m telescope.

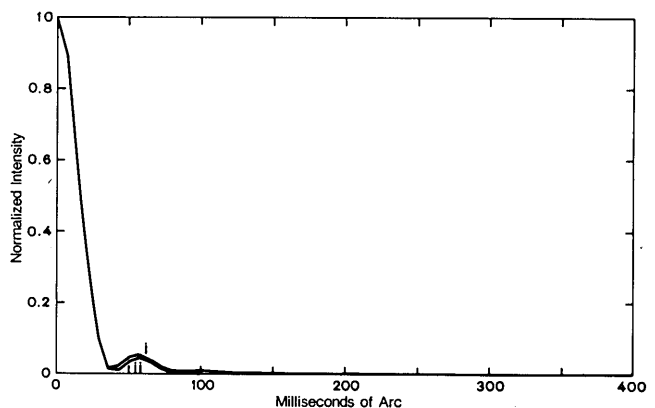


Fig. 2. Radial averaged profiles for (i) WSA/WD Gamma Orionis and (ii) Airy pattern of 3.8-m aperture with a 1:3 central obscuration at $\lambda = 650.0/0.2$ nm.

aperture and λ is the observing wavelength. This Gaussian is divided out, and the remaining bias of unity is subtracted. This effectively removes the photon-noise biased-induced photon spike from these images.

Figure 1 shows the radial averaged profiles for the SAA, WSA/XC, and WSA/WD images for the point-source Gamma Orionis observed at the Kitt Peak National Observatory (KPNO) 4-m Mayall telescope with a bandpass of 2.0 nm centered on 650.0 nm using the Steward Observatory (SO) speckle camera.¹³ Comparison of these profiles clearly shows the seeing-produced background in both the SAA and WSA/XC reductions to be substantially reduced to the flat background shown in the WSA/WD profile. Figure 2 compares the same WSA/WD result to that of an Airy profile for a 3.8-m aperture with a central obscuration ratio of 1:3, which is the case for the Mayall telescope. These two profiles compare very favorably: the width of the central lobe and the position and amplitude of the first Airy ring agree to within a few percent. Figure 3 shows the theoretical Airy pattern and the reconstructed Airy pattern image from which the radial-averaged profiles were computed. The rms difference between these two images is $\approx 0.2\%$ that of the peak for radii greater than the first Airy ring (the region where the seeing is dominant in the SAA and WSA/XC images). The effects of a nonuniform Airy pattern give an rms difference of $\sim 1.9\%$ for radii within the first Airy ring.

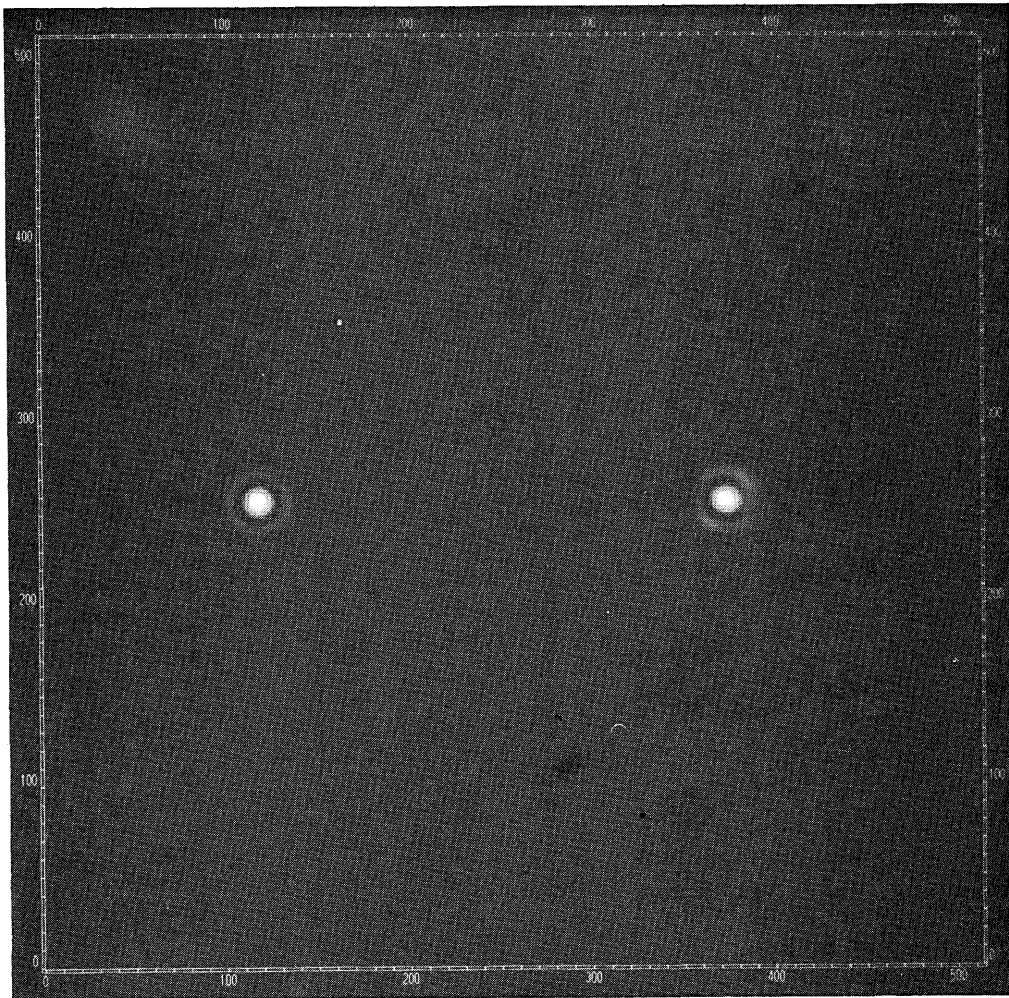


Fig. 3. (Left) Theoretical and (right) measured Airy patterns of the KPNO 4-m telescope. (See Fig. 2 for parameters.) Scale, 7.2 msa/pixel.

WSA/WD radial profiles for the extended object Alpha Orionis and the unresolved point sources Gamma and Epsilon Orionis, taken with the SO 2.3-m telescope, are shown in Fig. 4. The observing bandpass of 0.3 nm was centered on 854.2 nm. The point-source observations of Gamma and Epsilon Orionis bracketed the measurements of Alpha Orionis. They give similar profiles, the difference indicating a residual sensitivity of the technique to differences in the data sets. At $\lambda = 850$ nm the diffraction limit of the 2.3 m is 76 milliseconds of arc (msa) so that the ~ 42 -msa disk of Alpha Orionis¹⁴ remains unresolved, as is seen in the figure. The Alpha Orionis profile shows an extension, most probably due to the presence of a circumstellar gaseous envelope, up to a radius of ~ 300 msa. This measurement is commensurate with power-spectrum analysis of a 4-m data set at the same wavelength as reported by Goldberg *et al.*¹⁵ A circumstellar envelope has also been detected with a rotation shearing interferometer¹⁶ at an observing wavelength of 535 nm.

Reconstructed images of both Alpha Orionis and Gamma Orionis are shown in Fig. 5. These observations were taken with the KPNO telescope with bandpasses of 656.3/0.3 nm and 650.0/2.0 nm. The Gamma Orionis images show a lumpy Airy ring at a NE-SW position angle [Figs. 5b and 5e]. By comparison with the point source, Alpha Orionis is clearly resolved by this larger telescope (Figs. 5a and 5d),

and the images also show structure at the same position angle as the lumpy Airy ring.

In order to remove the effects of the lumpy point-spread function (PSF) from these Alpha Orionis images, we used the CLEAN¹⁷ algorithm. CLEAN has been successfully applied in the past to radio interferometric observations in order to remove artifacts and systematics due to the interfer-

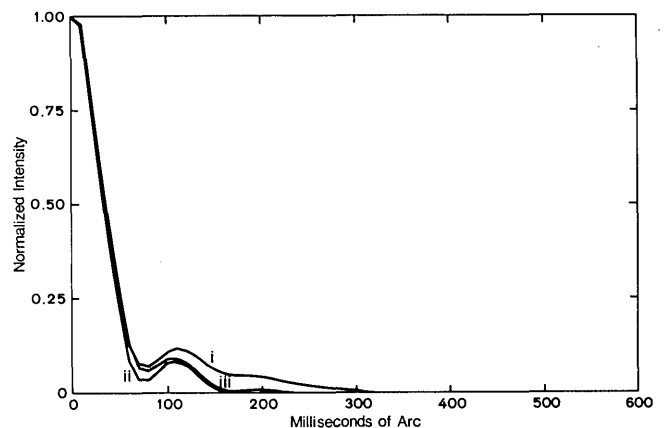


Fig. 4. WSA/WD radial averaged profiles of (i) Alpha Orionis, (ii) Epsilon Orionis, and (iii) Gamma Orionis taken with the Steward Observatory 2.3-m telescope at $\lambda = 854.2/0.3$ nm.

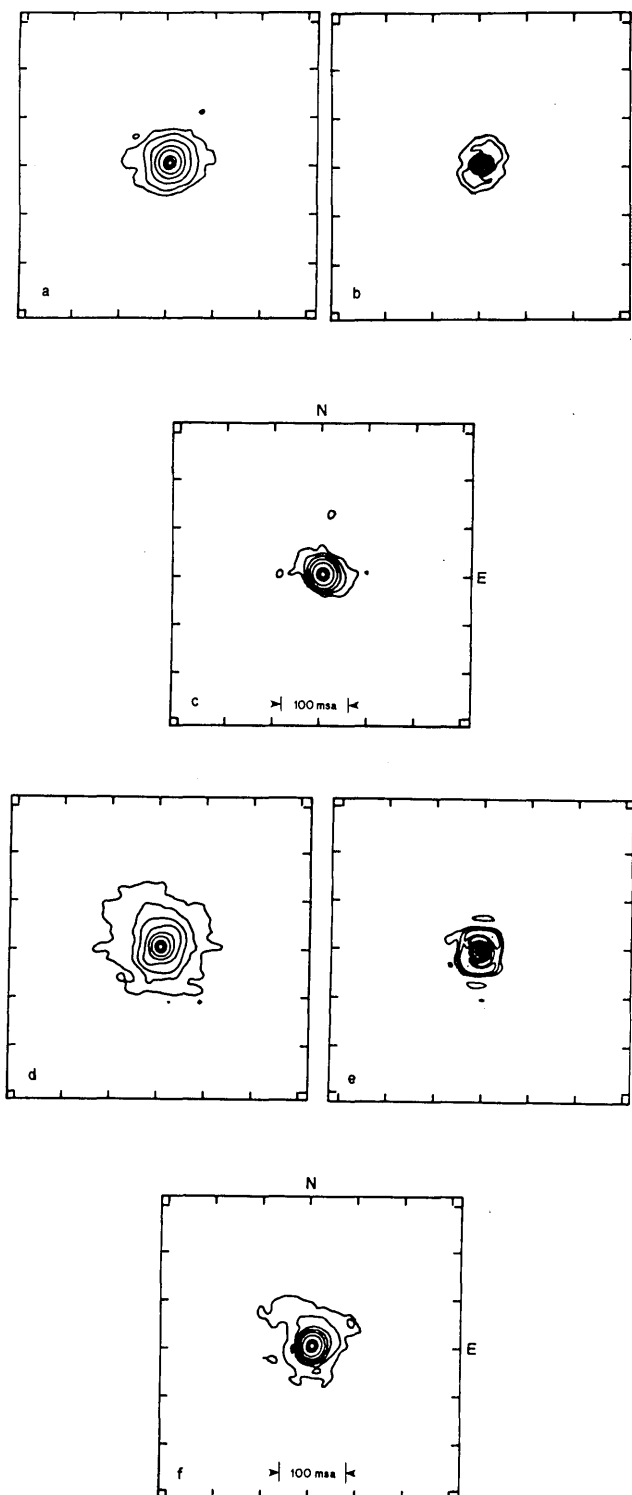


Fig. 5. Reconstructed images of Alpha and Gamma Orionis. a, WSA/WD Alpha Orionis ($\lambda = 656.3/0.3$ nm); b, WSA/WD Gamma Orionis ($\lambda = 656.3/0.3$ nm); c, a cleaned by b as described in text; d-f, as before but at $\lambda = 650.0/2.0$ nm. All observations at KPNO 4-m telescope.

ometer beam. It is an iterative process that locates the brightest pixel in the dirty map (resolved object image), and at this location it subtracts the dirty beam (point-source image), which is set to be a factor (loop gain, G) of the current peak in the dirty map. The process is repeated on

the residual. The algorithm generates an array of delta functions of varying intensities in such a way that the dirty map can be considered to be the weighted sum of the dirty beam at the delta-function locations plus the final residual. The iterations stop either when the intensity of the final residual is at the image noise level or when a certain number of negative delta functions is reached. The clean map is generated by convolving the delta-function array with a clean beam, which is usually obtained by fitting a Gaussian to the central component of the dirty beam. The quality of the final clean map depends on both the value of G and the number of iterations.

The cleaned images of Alpha Orionis are shown in Figs. 5c and 5f. The loop gain was set at 70%, and 50 iterations were used. These images show the removal of the lumpy Airy ring and indicate a nonuniform structure of the stellar envelope.

The use of CLEAN is further demonstrated in the next figure. A data set of Alpha Orionis and Epsilon Orionis taken with the SO 2.3-m telescope at a wavelength of 650 nm was reduced using the WSA/XC algorithm. These images are shown in Figs. 6a and 6b, respectively. They still include the photon spike, but the seeing background was removed by approximating it by a Gaussian and then subtracting. Both of these images contain, in addition to the noise spike, a video artifact due to the nonlinear response of the TV camera. This undershoot is produced by the video cassette recorder electronics after scanning across a bright speckle. The Epsilon Orionis image was used as a dirty beam to CLEAN the Alpha Orionis image (Fig. 6c) as described above. The loop gain was also set to 70% for 50 iterations. This clean image shows the removal of the undershoot artifact and also shows the presence of a probable stellar envelope with a position angle similar to that seen in the 4-m data set. The astrophysical interpretation of these

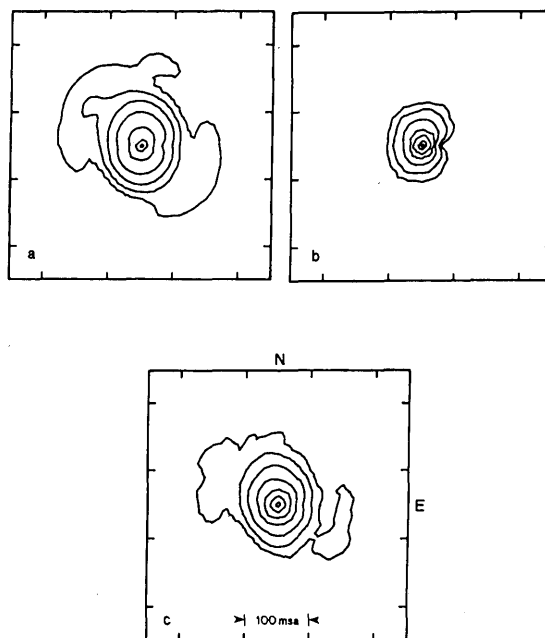


Fig. 6. Reconstructed images of Alpha and Gamma Orionis. a, WSA/XC Alpha Orionis; b, WSA/XC Gamma Orionis; c, a cleaned by b as described in text. Observations at SO 2.3-m telescope at $\lambda = 650.0/2.0$ nm.

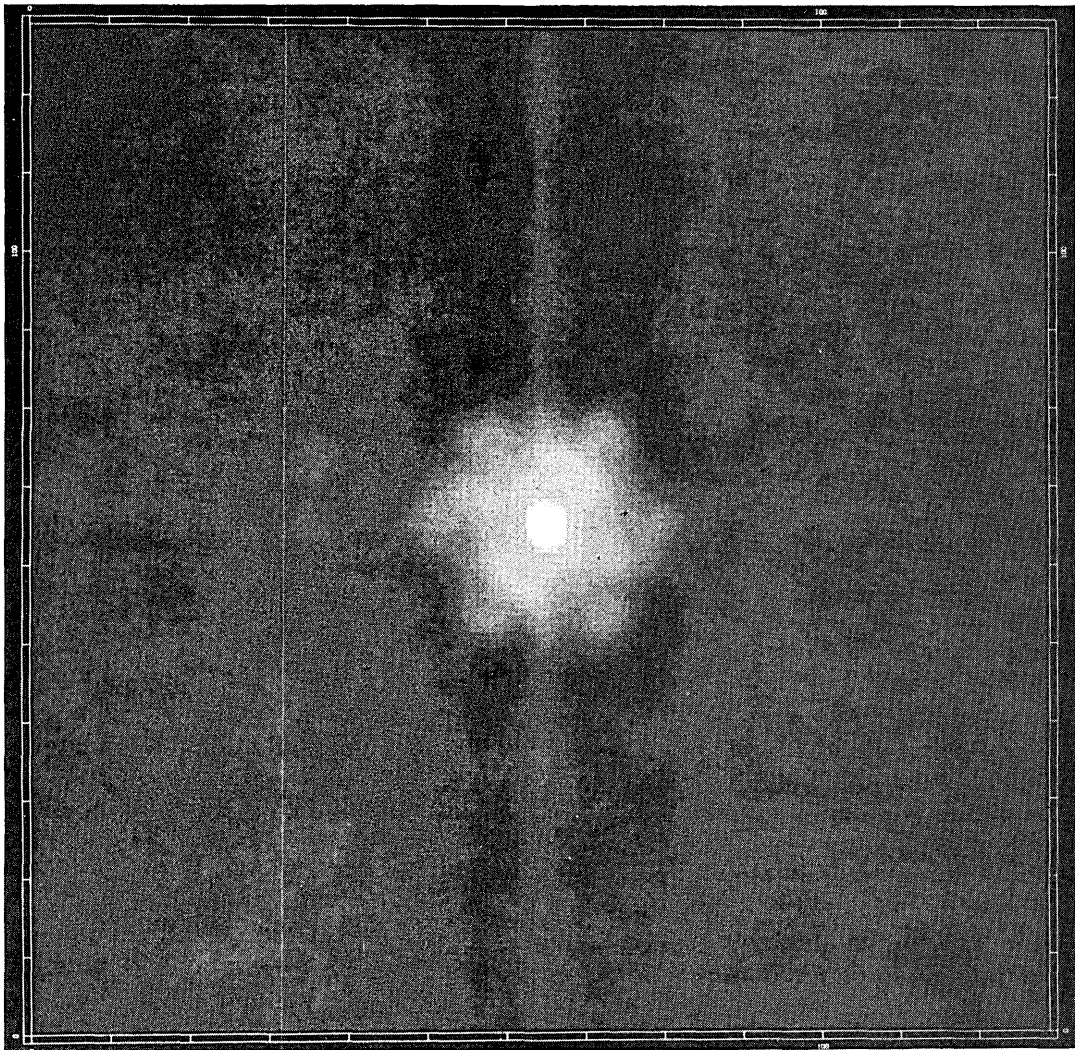


Fig. 7. WSA/WD image of Gamma Orionis taken with the fully phased MMT at $\lambda = 656.3/0.3$ nm. The artifacts are a result of the apodizing window caused by the video digitizer. This is the MMT PSF. Scale, 5 msa/pixel.

and other Alpha Orionis images is currently in preparation for publication elsewhere.¹⁸

Finally, Fig. 7 shows the PSF of the fully phased multiple mirror telescope (MMT) at a bandpass of 0.3 nm centered on 656.3 nm, using Gamma Orionis as an unresolvable source. The FWHM of the central lobe ≈ 20 msa, which is consistent with that of an Airy pattern for a 6.9-m aperture at the same wavelength. The sidelobes show the sixfold symmetry expected, but nonuniform amplitudes indicate imperfect phasing. The computed response published by Angel¹⁹ can be compared favorably with this result. The potential utility of the MMT as a phased-array high-resolution imaging telescope is discussed further by Hege *et al.*²⁰

DISCUSSION

The WSA technique appears to produce realistic PSF's for three telescopes, the SO 2.3-m, the KPNO 4-m, and the fully phased 6.9-m MMT. The results for the extended object, Alpha Orionis, agree between the 2.3 m and the 4 m when the different resolution limits are taken into account. The disk size and envelope presence agree well with other measurements. The major improvement of this technique over oth-

er SAA analyses is its apparent seeing self-calibration, which produces a flat background (i.e., no residual seeing bias), thus permitting realistic interpretation of extended low-power structure such as stellar envelopes. This self-calibration is due to the selection of all speckles and the weighting of the impulses so that there is no residual when a speckle is deconvolved by its corresponding impulse. The use of the CLEAN algorithm allows the systematics of the telescope PSF (and even serious video artifacts) to be removed when an unresolved point source (dirty beam) is observed.

Throughout this analysis it has been assumed that both the resolved and the unresolved objects produce object independent WSA/WD images. However, it was previously noted that SAA images are object dependent owing to the convolution of the diffraction-limited object with an object-dependent PSF.²¹ The latter term can arise for a number of reasons. The presence of Poisson noise in the data may affect the accuracy with which the speckle maxima are located. This will be especially true for low-contrast extended objects, and the net effect is a blurring of the final image. For the case of a binary star each speckle will have two maxima that lead to the presence of ghosts in the final image. The data presented in this paper consist of single maximum

high-contrast speckles and appear not to suffer from the effect of the object-dependent point-spread function. A new method of locating the speckle positions is needed for the cases of multiple-peaked objects and in the presence of strong Poisson noise. A matched-filter approach has been applied and is reported elsewhere.²² It is hoped that this will also allow extension of the WSA/WD analysis to the faint object (photon-limited) domain, e.g., quasi-stellar objects and galactic nuclei.

The results presented here represent a preliminary analysis of a much larger data base, which is currently being studied for astrophysical content.¹⁸

ACKNOWLEDGMENTS

We wish to thank Andreas Eckart for the application of the CLEAN algorithm. We would also like to thank R. H. T. Bates for many useful discussions, which enabled us to understand the properties of SAA images.

The research of E. Ribak is supported by a Weizmann Fellowship. This work was supported in part by Air Force Geophysics Laboratory contract F19628-82-0025, U.S. Air Force Office of Scientific Research grant 82-0020, and National Science Foundation grants AST-8201092 and AST-8312976.

Observations reported here were obtained at the Multiple Mirror Telescope Observatory, a joint facility of the University of Arizona and the Smithsonian Institution, and at Kitt Peak National Observatory.

Kitt Peak National Observatory is a division of the National Optical Astronomy Observatories, operated by the Association of Universities for Research in Astronomy, Inc., under contract to the National Science Foundation.

* Visiting Astronomer from Department of Astronomy, New Mexico State University, Las Cruces, New Mexico 88003.

† Visiting Astronomer at Kitt Peak National Observatory.

REFERENCES

1. A. Labeyrie, "Attainment of diffraction limited resolution in large telescopes by Fourier analyzing speckle patterns in a star image," *Astron. Astrophys.* **6**, 85 (1970).
2. J. R. Fienup, "Phase retrieval algorithms: a comparison," *Appl. Opt.* **21**, 2758 (1982).
3. R. H. T. Bates and W. R. Fright, "Composite two-dimensional phase restoration procedure," *J. Opt. Soc. Am.* **73**, 358 (1983); "Reconstructing images from their Fourier intensities," in *Advances in Computer Vision and Image Processing*, T. S. Huang, ed. (JAI, Greenwich, Conn., 1984, vol. 1, Chap. 5).
4. S. F. Gull and G. J. Daniell, "Image reconstruction from incomplete and noisy data," *Nature* **272**, 686 (1978).
5. C. R. Lynds, S. P. Worden, and J. W. Harvey, "Digital image reconstruction applied to Alpha Orionis," *Astrophys. J.* **207**, 174 (1976).
6. R. H. T. Bates and F. W. Cady, "Towards true imaging by wideband speckle interferometry," *Opt. Commun.* **32**, 365 (1980).
7. K. T. Knox and B. J. Thompson, "Recovery of images from atmospherically degraded short-exposure photographs," *Astrophys. J.* **193**, L45 (1974).
8. R. H. T. Bates, "Astronomical speckle imaging," *Phys. Rep.* **90**, 203 (1982).
9. J. C. Dainty, "Stellar speckle interferometry," in *Laser Speckle and Related Phenomena*, Vol. 9 of Topics in Applied Physics (Springer-Verlag, Berlin, 1984), Chap. 7.
10. B. R. Hunt, W. R. Fright, and R. H. T. Bates, "Analysis of the shift-and-add method for imaging through turbulent media," *J. Opt. Soc. Am.* **73**, 456 (1983).
11. W. G. Bagnuolo, "The application of Bates' algorithm to binary stars," *Mon. Not. R. Astron. Soc.* **200**, 1113 (1982).
12. W. G. Bagnuolo, "Image restoration by the shift-and-add algorithm," *Opt. Lett.* **10**, 200 (1985).
13. E. K. Hege, E. N. Hubbard, P. A. Strittmatter, and W. J. Cocke, "The Steward Observatory speckle interferometry system," *Opt. Acta* **29**, 701 (1982).
14. A. Y. S. Cheng, P. A. Strittmatter, E. K. Hege, E. N. Hubbard, L. Goldberg, and W. J. Cocke, "Diameter and limb-darkening measures for Alpha Orionis," submitted to *Astrophys. J.*
15. L. Goldberg, E. K. Hege, E. N. Hubbard, P. A. Strittmatter, and W. J. Cocke, "Speckle interferometry of Alpha Orionis: preliminary results," in *Second Cambridge Workshop on Cool Stars, Stellar Systems and the Sun*, M. S. Giampapa and L. Golub, eds., SAO Special Report 392 (Smithsonian Astrophysical Observatory, Cambridge, Mass., 1982), Vol. 1, p. 131.
16. C. Roddier and F. Roddier, "High angular resolution observations of Alpha Orionis with a rotation shearing interferometer," *Astrophys. J.* **270**, L23 (1985).
17. J. A. Högbom, "Aperture synthesis with a non-regular distribution of interferometer baselines," *Astron. Astrophys. Suppl.* **15**, 417 (1974).
18. J. C. Hebden, J. C. Christou, A. Y. S. Cheng, E. K. Hege, P. A. Strittmatter, J. M. Beckers, and H. P. Murphy, "Two dimensional images of Alpha Orionis," submitted to *Astrophys. J.*
19. R. P. Angel, "Very large ground-based telescopes for optical and IR astronomy," *Nature* **295**, 651 (1982).
20. E. K. Hege, J. M. Beckers, P. A. Strittmatter, and D. W. McCarthy, "The multiple mirror telescope as a phased array telescope," *Appl. Opt.* **24**, 2565 (1985).
21. M. J. McDonnell and R. H. T. Bates, "Digital restoration of an image of Betelgeuse," *Astrophys. J.* **208**, 443 (1976).
22. E. Ribak, E. K. Hege, and J. C. Christou, "The use of matched filters to identify speckle locations," *Proc. Soc. Photo-Opt. Instrum. Eng.* **556**, 196 (1985).